Transactions of the Korean Nuclear Society Spring Meeting
Jeju, Korea, May 29-30, 2014

A Sensitivity Study on the Radiation Shield of KSPR Space Reactor

Š. Čerba[a,b], Hyun Chul Lee[a*], Hong Sik Lim[a], Jae Man Noh[a],
[a]*Korea Atomic Energy Research Institute, Daedeok-Daero 989-111, Yuseong-Gu, Daejeon, Korea*
[b]*INPE, FEIT, Slovak University of Technology in Bratislava, Ilkovicova 3, 812 19, Bratislava, Slovakia*
[*]*Corresponding author:*lhc@re.kaeri.kr

1. Introduction

Nuclear power plants are considered to be one of the most cost-effective and reliable power sources for electricity generation. As a result of advances in nuclear research, even several new applications are offered for the utilization of nuclear energy. Some reactors are used for research purposes and the Gen IV reactors offer some possibilities also for non-electric applications. Apart from the most common fields, the nuclear reactors could be used even for some unconventional applications. One of these fields is the possibility to use a nuclear reactor as a power supplier for deep space probe or orbiter. Unlike the "terrestrial ones" the space reactors have to meet several specific technical requirements. They must be safe, simple, compact, as well as easy to operate while the electronic part of the space station has to be protected against ionizing radiation. The idea of a space reactor was realised some decades ago and since that time several research activities have been performed into this field. The US National Aeronautics and Space Administration (NASA) has been developing a small fast reactor called as fission power system (FPS) for deep space mission, where highly enriched uranium (HEU) is used as fuel [1]. On the other hand, other researchers have also surveyed a thermal reactor concept with low enriched uranium (LEU) for space applications [1-5]. One of the main concerns in terms of a space reactor is the total size and the mass of the system including the reactor itself as well as the radiation shield. Since the reactor core is a source of neutrons and gamma photons of various energies, which may cause severe damage on the electronics of the space stations, the questions related to the development of a radiation shield should be address appropriately. The proposal of a radiation shield for a small space reactor is discussed in this paper. The requirements for the radiation shield have been addressed in terms of maximal absorbed doses and neutron flounces during 10 years of operation.

2. Description of the System

The Korean Space Power Reactor (KSPR) [5] is being studied at Korea Atomic Energy Research Institute (KAERI) as a possible power supplier for deep space probe or orbiter. A preliminary design of the reactor core has already been proposed. The proposed reactor core consists of 34 hexagonal fuel assemblies filled with low enriched U metal and $ZrH_{1.5}$ moderator ensuring the moderator to fuel ratio 15. The reactor power is 5 kW_{th} and the operation temperature is 1100 K. The cooling is ensured through a two-way heat pipe mechanism with NaK cooling fluid. The reactor control is ensured through the system of three control rods with natural boron carbide. The control rods are introduced from the top axial reflector. The axial and radial reflectors are made of Be. The reactor core was developed to have appropriate performance for 10 years of continuous reactor operation without the necessity of refuelling or any sort of human intervention. The top and front views of the reactor core are shown in Fig.1 and Fig.2. The basic core parameters are summarized in Table I.

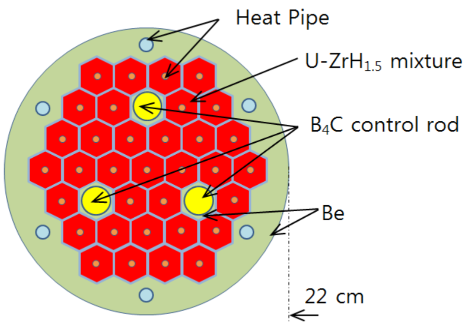

Fig.1 The top view of the reactor core

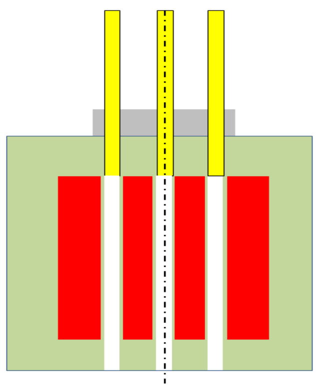

Fig.2 The front view of the reactor core

Table I Basic core design parameters

Reactor thermal power	5 kW_{th}
Operation temperature	1100 K
Fuel type	U metal

Fuel enrichment	19.95 $\%_w$
Coolant	NaK
Number of fuel Blocks	34
Moderator	$ZrH_{1.5}$
Core height	36.6 cm
Axial reflector thickness	3.7 cm
Reflector ~~Outer~~ outer radius	22 cm
Effective core radius	15.65 cm
Fuel Block flat-to flat	4.8 cm
Control rod material	Natural B_4C
Absorber radius	2.2 cm
Inner/outer heat pipe radius	0.55/1cm
Reflector	Be

The aim of this study is to propose a neutron and photon shield to keep the absorbed doses of a 1 cm thick 4.5 m wide Si disc target at 10 m from the reactor below 250 Gy during 10 years of operation. Since this reactor is designed for space application, the most important criterion is the total mass of the shield. The simplified model of the described system is shown in Fig. 3.

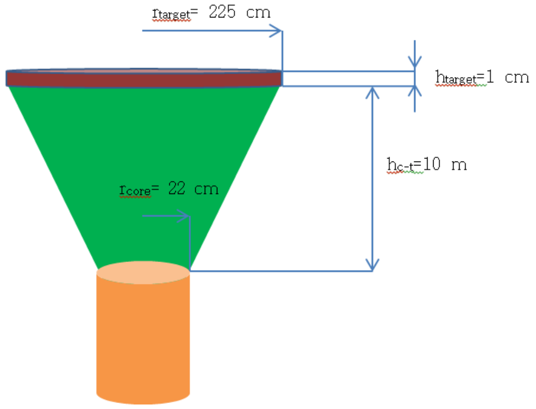

Fig.3 The ~~Simplified~~ simplified ~~Model~~ model of the ~~System~~system

3. Theoretical background

For a given volume of matter of mass m, the energy imparted ε in some time interval is the sum of the energies (excluding rest-mass energies) of all charged and uncharged ionizing particles entering the volume minus the sum of the energies (excluding rest-mass energies) of all charged and uncharged ionizing particles leaving the volume of material. This energy is eventually degraded almost entirely into thermal energy. The specific energy which represents the energy imparted per unit mass, leads to the absorbed dose (Eq.1) [6].

$$D = \lim_{m \to 0} \frac{d\bar{\varepsilon}}{dm} \tag{1}$$

The basic unit of the absorbed dose is 1 Gy representing 1 J of energy per 1 kg of material. It is also common to use 1 rad as the unit of the absorbed dose (rad as Radiation Absorbed Dose). The conversion between these units is as follows: 1 Gy = 100 rad. In case of an MCNP calculation the F6:n,p tallies are intended to calculate the absorbed doses. The physical quantity represented by the F6 tally can ~~represents~~ be thought as the total cross section $\sigma_t(E)$ multiplied by the average heating number $H(E)$ and the angular flux $\Psi(\vec{r},\vec{\Omega},E,t)$ integrated through the cell volume, particle energy and time, normalized to be per unit cell mass. [6,7] The F6 cell heating tally is a track length flux tally modified to tally a reaction rate convolved with an energy-dependent heating function instead of a flux. In general MCNP calculates the F6 tally using Eq.2 [7],

$$F6 = WT_l\sigma_t(E)H(E)\frac{\rho_a}{m} \tag{2}$$

where W is the particle weight, T_l the particle track length (cm), $\sigma_t(E)$ the energy dependent total microscopic cross section, $H(E)$ the energy dependent heating number (MeV/collision), ρ_a the atom density (atoms/barns.cm) and m the cell mass (g). The unit of the heating tally is MeV/g, hence one may use Eq.3 to obtain the absorbed dose in units of J/kg. The final quantity is obtained after a multiplying by the appropriate source term.

$$\dot{D} = S.F6:n(p).N \tag{3}$$

The linear interaction coefficient for indirectly ionizing radiations such as gamma rays or neutrons, $\mu(E)$, also called the macroscopic cross section $\Sigma(E)$, in the limit of small distances, is the probability per unit distance of travel that a particle of energy E experiences an interaction such as scattering or absorption. From this definition, it can be easily shown that the probability of a particle traveling a distance x without interaction is given by Eq. 4. [6]

$$P(x) = e^{-\mu x} \tag{4}$$

In this equation μ is called linear attenuation factor in case of photons and removal cross-section in case of neutrons. From this result, the half-value thickness HVT that is required to reduce the uncollided radiation to one-half of its initial value can readily be found, namely by Eq. 5 [6].

$$HVT = \frac{-\ln 2}{\frac{d\ln(A_f(x))}{dx}} \tag{5}$$

The concept of half-value thicknesses, although stated here for uncollided radiation, is also often used to describe the attenuation of the total radiation dose. The photon source and the attenuating medium, the energy spectrum of the total photon flounce at some point of interest may be divided into two components. The unscattered component $D^0(r)$ consists of just those photons that have reached the given distance from the source without having experienced any interactions in the attenuating medium. The scattered component $D^S(r)$ consists of source photons scattered one or more times, as well as secondary photons such as X-rays and annihilation gamma rays. Accordingly, the dose or detector response at point of interest may be divided into unscattered (primary) and scattered (secondary) components. The build-up factor *B(r)* is defined as the ratio of the total dose to the unscattered dose and can be expressed by Eq.6 [6].

$$B(r) = \frac{D(r)}{D^0(r)} \qquad (6)$$

4. Calculation scheme and method

For this analysis the multi-purpose stochastic MCNP [7] code was selected. In case of MCNP the investigation of the radiation shield performance can be performed either in a direct or an indirect way. In case of the direct calculation a KCODE criticality calculation is performed and the doses are calculated by setting up F6 neutron and photon tallies. The advantage of this method is that only one calculation is required, however in case of a KCODE problem the neutron source distribution is changing until a reliable convergence is achieved; therefore the tally results are strongly influenced by the convergence of the fission source. The indirect way requires two calculations, a KCODE criticality calculation and a coupled neutron photon fixed source calculation. The criticality calculation serves to determine the neutron source, which is used for the fixed source calculation where the tally scores are collected. A fixed source calculation uses the pre-defined neutron source, which is not changing during the calculation, and performs the particle transport by tracking a defined number of particles until they are killed or they leak out the system. In this study the indirect way was used, where the neutron source was defined through the MCNP SDEF card using the tally results obtained from the previous criticality calculation. The MCNP source term requires the knowledge of the spatial, angular, time and energy distribution of the neutron source. In order to apply the features of the MCNP SDEF card it should be assumed the core of the reactor is of cylindrical shape, although it was a hexagon in our case. The radial and axial probability distributions of the neutron flux were found by utilizing a smooth grid of cylindrical MCNP mesh tallies. Then the discrete tally results were used to define the probability density function of the neutron source. The neutron spectrum was tallied by utilizing a multi-group energy structure. The comparisons of the original and the tallied source definitions, in terms of the radial probability distribution function and the neutron spectrum is shown in Fig.4 and Fig.5. On the pictures "kcode" stands for the tally results from the criticality calculation, and "fixed" for the tally results from the fixed source calculation with the source taken from the "kcode" case.

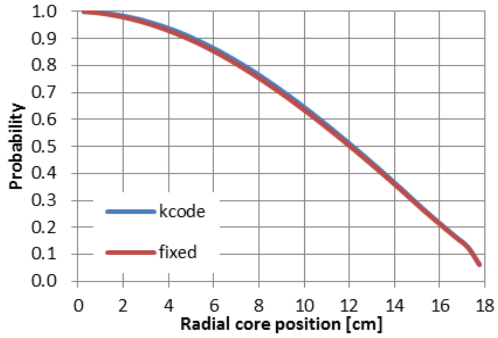

Fig.4 Comparison of the radial probability distribution functions

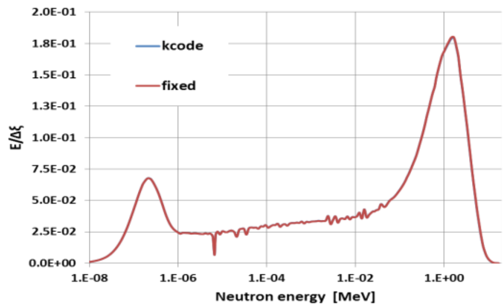

Fig.5 Comparison of the neutron spectra

The comparison showed very good agreement, with an average standard deviation at the level of 0.1 %. The comparisons of the axial probability distribution and the spectra showed similar performance. Although there were some energy groups with large relative errors however their influence on the total result could be concluded as negligible and therefor it was justified to utilize the presented calculation scheme.

5. Calculation results

7.1. Comparison with a fast reactor system

The NASA has proposed a small fast reactor called fission power system.[1] This fast reactor utilizes 93 % enriched disk type UMo metallic fuel with NaK coolant pipes and BeO reflector. The reactivity control is assured through a 90 % enriched B_4C control rod introduced from the bottom reflector and a safety scholar placed between the core bundle and the radial reflector. The radiation shield consists of several layers of LiH and W. The thermal power of this system is 13 kW_{th} and the operation temperature is assumed to be 1200 K. The biggest advantage of this reactor concept is the very low core and shield mass, 133kg and 271kg respectively [1]. Table II shows a comparison of the neutron sources and average values of neutron and photon fluxes per 1 kW_{th} reactor power for the KSPR and a fast system which was modelled based on the design parameters listed in reference 1.

Table II Comparison of the neutron and photon fluxes

Reactor	KSPR	Fast System
S [n/s]	8.43E+13	8.80E+13
φ_n^{core} [cm^{-2}s^{-1}]	7.87E+10	2.19E+11
φ_p^{core} [cm^{-2}s^{-1}]	6.39E+10	9.12E+10
$\varphi_n^{core}/\varphi_n^{total}$	0.552	0.706
$\varphi_p^{core}/\varphi_p^{total}$	0.448	0.294
φ_n^{ref} [cm^{-2}s^{-1}]	2.69E+10	8.39E+10
φ_p^{ref} [cm^{-2}s^{-1}]	1.84E+10	2.44E+10

Due to the higher fission rate in the fast neutron spectrum the neutron source in case of the fast system is about 4 % higher. Due to the higher parasitic neutron capture and inelastic scattering on ^{238}U higher photon production can be observed in case of the thermal reactor. This fact may strongly influence the proposal of the radiation shielding since more photon attenuating material would be needed to meet the radiation limits in comparison with the fast reactor. The comparisons of the distributions of the neutron and photon fluxes in different positions from the reactor core are shown in Fig.6 and Fig.7. For a more realistic comparison the same reflector thickness of 7 cm was used in case of both reactors. As it is obvious the reflector in case of the fast reactor (noted as fast in the figures) shows better performance either for neutrons or photons compared with the KSNP(noted as thermal in the figures), since the decrease of the flux is much steeper. This behaviour can be explained by the difference in the neutron and photon flux.

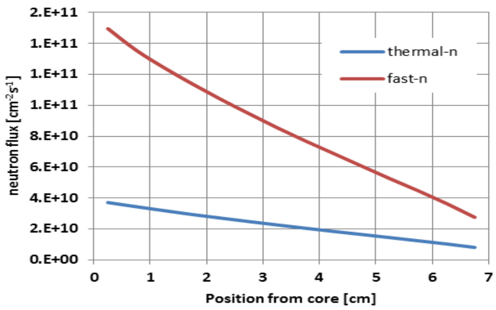

Fig.6 Comparison of the neutron fluxes

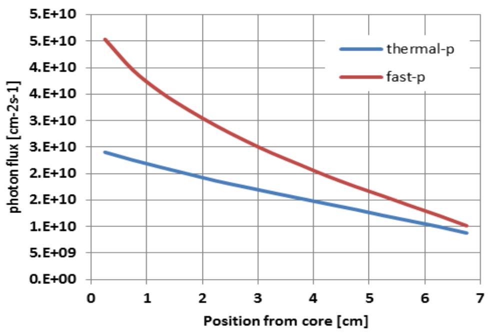

Fig.7 Comparison of the photon fluxes

To assess the effectiveness of the reflector of the KSPR reactor design in terms of neutron and photon attenuation a comparative study was performed between the two reactors. In this study the neutron and photon fluxes were tallied before entering and after leaving the axial reflector. In case of the KSPR thermal reactor three cases were investigated. The "basic" case utilizing 3.7 thick Be reflector and 2 cases with 7 cm thick Be and BeO reflectors respectively. In each case the effectiveness of the reflector was calculated as the ratio of in/out flux and in/out flux per unit thickness. The results can be found in Table III and Table IV.

Table III. Comparison of the reflector effectiveness for neutron attenuation

Core and reflector	In/Out	In/Out/1cm
Fast System 7 cm Be	8.65	1.24
KSPR 3.7 cm Be	3.81	1.03
KSPR 7 cm Be	6.29	0.90
KSPR 7 cm BeO	6.63	0.95

Table IV. Comparison of the reflector effectiveness for photon attenuation

Core and reflector	In/Out	In/Out/1cm
Fast System 7 cm Be	4.18	0.60
KSPR 3.7 cm Be	1.81	0.49
KSPR 7 cm Be	2.46	0.35
KSPR 7 cm BeO	3.00	0.43

It can be seen that the best effectiveness either in terms of neutron or photon attenuation was found in case of the fast reactor. The efficiency of the basic KSPR shield was 2.3 times lower in comparison with the fast system. This value could be reduced by increasing the reflector thickness to be the same as in the fast system; however the efficiency would be still 1.4 lower. On the other hand, by increasing the reflector thickness the efficiency per unit thickness was decreased and even the neutron performance of the core was influenced. A slight difference can be seen between the Be and BeO reflectors, however the better performance of the BeO is devaluated by the higher density of BeO.

7.2. Investigation of the effectiveness of various attenuation materials

The investigation of the effectiveness of various shielding materials was performed on the core model depicted on Fig.8. Seven materials were investigated, namely LiH, Be, BeO, $ZrH_{1.5}$, W, Pb and depleted U, while the shielding mass was kept constant in all cases. In the basic case the shield was homogenously filled with LiH and the height was set to be equal to the upper position of the withdrawn control rods. The volume of this cone can be calculated using Eq.7 and the radius of the top base of the cone by Eq.8.

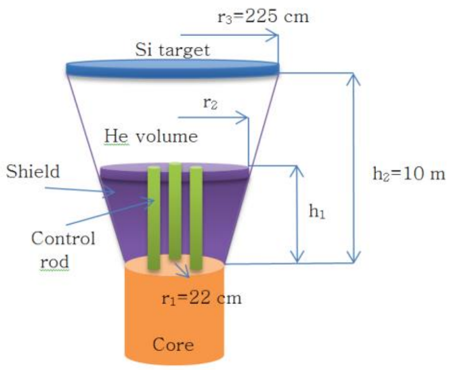

Fig.8 The front view of the used core model

$$V_{cone} = \frac{1}{3}\pi\left(r_1^2 + r_2^2 + r_1 r_2\right)h_1 \quad (7)$$

$$r_2 = r_1 + \frac{r_3 - r_1}{h_2} h_1 \quad (8)$$

In order to keep constant shielding mass for materials with different density the shielding volume has to be modified; however this volume is a function of two unknowns, r_2 and h_1. The h_1 parameter can be expressed by Eq.9 which is a cubic equation.

$$A^3 h_1 + B^2 h_1 + C h_1 + D = 0 \quad (9)$$

By solving this equation the h_1 and r_2 parameters can be easily found. The calculated parameters with the corresponding volumes can be found in Table V.

Table V. Basic parameters of the shield design

material	r_2 [cm]	h_1 [cm]	ρ [g.cm^{-3}]	V_{cone} [cm^{-3}]
LiH	31.74	40.30	0.780	92424.6
Be	26.31	21.23	1.848	39010.4
BeO	24.82	13.89	3.010	23950.6
$ZrH_{1.5}$	23.60	7.88	5.600	12873.4
W	24.49	2.24	19.150	3764.6
Pb	22.82	4.03	11.340	6357.3
Dep.U	22.51	2.53	18.330	3933.0

For each material a separate calculation was performed with a focus on the absorbed doses at a 1 cm thick Si target placed 10 m from the reactor core. The results were compared with the case when the shielding volume was simply replaced by He, assuming no significant particle attenuation. To assess the effectiveness of the given materials a C_i coefficient has been introduced, which can be calculated using Eq.10.

$$C_i = \frac{D_{He}}{D_i m_i} \quad (10)$$

In this equation D_{He} stands for the dose in a case without shielding (replaced by He), D_i for the dose in case of i-th material and m_i is the mass of i-th material. The results can be found in Table VI.

Table VI Comparison of the effectiveness of various shielding materials

Material	D_t [Gy]	C_{ni}[kg^{-1}]	C_{pi} [kg^{-1}]
He	16039.2	-	-
LiH	6924.0	10.4001	0.0305
Be	5643.0	0.0543	0.0389
BeO	6378.2	0.2897	0.0333
$ZrH_{1.5}$	5605.7	0.1054	0.0384
W	5218.6	0.0192	0.0455
Pb	3961.3	0.0173	0.0637
Dep. U	4259.1	0.0174	0.0584

The results are showing very good performance of LiH for neutron attenuation. Its effectiveness is almost 2 orders of magnitude better than the effectiveness of the other investigated material. In terms of photon attenuation, the difference between various materials was not so significant. As we expected, the best performance was found in case of heavy nuclides. Although Pb showed the best effectiveness for photon attenuation, due to low melting point of Pb, LiH and W were chosen as basic materials.

7.3. Application of the principle of half value thickness

To find the appropriate thickness of the radiation shield, the principle of the half value thickness may be useful. The half value thickness (HVT) represents the thickness of material that can reduce the absorbed doses by a factor of 2. To find the HVT value for LiH and W two separate calculations were performed, where the shield was replaced by a single volume of the given material and the axial distribution of the neutron flux was tallied. The results were graphically plot and exponential fit was used to find the linear attenuation coefficient or the removal cross section, which are proportional to the HVT value. The plots of the neutron fluxes are shown in Fig.9 and Fig.10 and the results are summarized in Table VII.

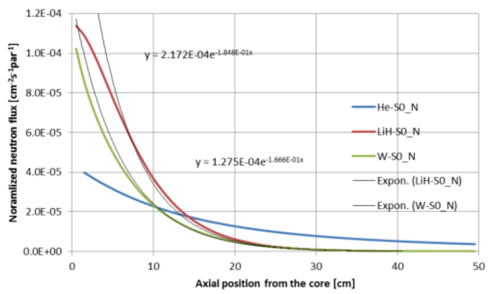

Fig.9 The distribution of the neutron flux in the shield

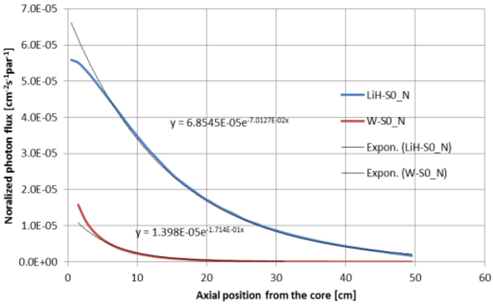

Fig.10 The distribution of the photon flux in the shield

Table VII. HVT values for various shielding materials

Material	HVT_n [cm]	HVT_p [cm]
LiH	3.75	9.88
W	4.15	3.01

On the basis of the achieved results a multi-layer design consisting of 5 cm thick LiH and 3 cm thick W has been chosen. The selected design for the reactors is shown in Fig. 11.

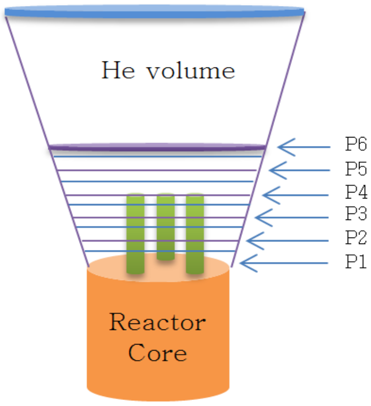

Fig.11 Shielding configurations of the space reactor design

The results are sown in Table VIII and Table IX. For the KSPR reactor the best performance was found in case of 3 shield elements placed at position P2 with the thickness of the third W layer reduced by 0.9 cm. The mass of this shield was 352.9 kg. Although there were some cases that could reduce the absorbed doses to lower values, they would require more material, thus the total weight of the shield would be higher. In case of the fast reactor, two shield segments placed at position P3 with additional 0.2 cm of W required the lowest shielding mass, 292.81 kg. It is obvious for the same reactor power the fast system required 60 kg less shielding material. This decrease may have been caused by different behaviour of shielding material in case of different neutron and photon spectra.

Table VIII. Comparison of various shield designs for the KSPR space reactor

Case	# of Shield Elements	Shield Element Position	D_t [Gy]	m [kg]
1	0	-	16459.5	0.0
2	1	P1	3478.4	100.3
3	2	P1~P2	881.8	215.7
4	3	P1~P3	228.0	347.2
5	4	P1~P4	66.5	495.7
6	5	P1~P5	19.6	662.4
7	2	P2~P3	632.7	246.8
8	2	P3~P4	548.2	280.0
9	3	P2~P4	153.3	395.4
10*	3	P2~P4	252.6	352.9

* : The thickness of the third W layer was reduced by 0.9 cm

Table IX. Comparison of various shield designs for the fast reactor

Case	# of Shield Elements	Shield Element Position	D_t [Gy]	m [kg]
1	0	-	4944.74	0.0
2	1	P1	470.54	219.4
3	2	P1~P2	126.72	352.8
4	3	P1~P3	31.67	503.2
5	4	P1~P4	15.27	671.8
6	5	P1~P5	87.42	401.1
7	2	P2~P3	337.22	250.6
8	2	P3~P4	318.01	283.8
9	3	P2~P4	221.83	298.3
10*	3	P2~P4	244.89	292.8

* : The thickness of the third W layer was increased by 0.2 cm

7.3. Investigation of the influence of the shielding mass on the reactor power

The aim of this part was to find out, whether the shielding mass changes linearly with the thermal power of the reactor. For each power level a new shield design was proposed that could meet the limits of the absorbed dose. The results of this analysis are shown in Table X and the shielding mass vs. reactor thermal power is plot on Fig. 12. The results are clearly showing that the shielding mass is not directly proportional to the reactor thermal power. The higher the power of the reactor is the lower the required mass per unit power is. While at 2 kW_{th} power level 93.6 kg of shield was required per unit power, but at 20 kW_{th}, it was only 22.85 kg. This phenomenon can be explained by different shield efficiency in case of deeper penetrations, caused by changes of the neutron and photon spectra.

Table X. Results of the shielding calculations at various power levels

Pow. [kW_{th}]	D_t [Gy]	Mass [kg]	C_m [kg/kW_{th}]
2.0	238.3	187.19	93.60
5.0	244.7	288.62	57.72
9.0	241.3	356.85	39.65
13.0	244.3	379.45	29.19
20.0	247.1	456.92	22.85

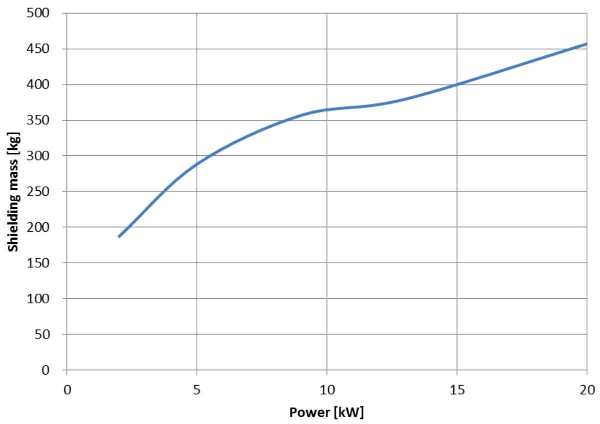

Fig.12 Influence of the reactor thermal power on the shielding mass

6. Conclusions

In this study s radiation shield design for a small space reactor was investigated. All the presented calculations were performed using the multi-purpose stochastic MCNP [7] code with temperature dependent continuous energy ENDF/B VII.0 [8] neutron and photon cross section libraries. The aim of this study was to design a neutron and gamma shield that can meet the requirements of 250 Gy absorbed during 10 years of reactor operation. The comparison with a fast reactor design showed that high content of ^{238}U strongly influences the shielding mass. This phenomenon is due to the higher photon production in case of the KSPR design and therefore the use of high ^{235}U enrichments and the operation in fast neutron spectrum may be more desirable. In case if the KSPR space reactor the best shielding performance was achieved while utilizing a multi-layer design combining 5 cm thick LiH and 3 cm thick W layers. It can be also concluded that the shielding mass is strongly dependent on the reactor thermal power, thus the highest efficiency in terms of shielding mass per unit of thermal power can be achieved in case of high reactor power.

REFERENCES

[1] Poston, D.I. et al.: A Simple, Low-Power Fission Reactor for Space Exploration Power Systems, Proc. of Nucl. and Emerging Tech. for Space 2013, Albuquerque, NM, February 25-28, 2013, NASA/TM—2011-217099.

[2] Teruhiko Kugo, et al., Design Study of Nuclear Power Systems for Deep Space Explorers (1) Criticality of Low Enriched Uranium Fueled Core, Proceedings of ICAPP ’09 Tokyo, Japan, May 10-14, 2009.

[3] Takaaki Nishiyama, et al., Proposal of Space Reactor for Nuclear Electric Propulsion System, Proceedings of ICAPP ’09 Tokyo, Japan, May 10-14, 2009.

[4] Paolo Venneri and Yonghee Kim, Feasibility of Low Enriched Uranium Fuel for Space Nuclear Propulsion, Trans. of the Korean Nuclear Society Spring Meeting Gwangju, Korea, May 30-31, 2013.

[5] Cerba, S. et al: A Feasibility and Optimization Study on a Small Space Reactor with 20w/o Uranium Fuel, Transactions of the Korean Nuclear Society Autumn Meeting Gyeongju, Korea, October 24-25, 2013.

[6] Cacuci, D.G. et al: Handbook of Nuclear Engineering, Chapter 11 - J. K. Shultis, R. E. Faw: Radiation Shielding and Radiological Protection (p.1316-1356), DOI 10.1007/978-0-387-98149-9_11, Springer Science+Business Media LLC 2010.

[7] X-5 Monte Carlo Team, 2004, MCNP5 General Monte Carlo N-Particle Transport Code, Version 5, LA-UR-03-1987.

[8] Chadwick, M. B., Obložinský, P., Herman, M.,: "ENDF/B-VII.0: Next Generation Evaluated Nuclear Data Library for Nuclear Science and Technology," Nuclear Data Sheets, vol. 107, no. 12, p. 2931 – 3060, 2006.